A novel approach for generalising walking gaits across embodiments and behaviours

A Novel Approach for Generalising Walking Gaits across Embodiments and Behaviours

Hsiu-Chin Lin[1], Matthew Howard[2], and Sethu Vijayakumar[1]

***Abstract*— Our goal is to introduce a more appropriate method of generalising walking gaits across different subjects and behaviours. Walking gaits are a result of complex factors that include variations resulting from embodiments and tasks, making techniques that use average template frameworks suboptimal for systematic analysis. The proposed work aims to devise methodologies for being able to represent gaits and gait transitions such that optimal policies may be recovered. The problem is formalised using a walking phase model, and the nullspace learning method is used to generalise a consistent policy. This policy can serve as reference guideline to quantify and identify pathological gaits. We have demonstrated robustness of our method with motion-capture data with induced gait abnormality. Future work will extend this to kinetic features and higher dimensional features.**

I. Introduction

Human walking is influenced by many factors, namely, (i) the embodiment of the subject (e.g., limb lengths), (ii) the environment in which the behaviour is performed (e.g., flat/uneven terrain) and (iii) task contextual factors (e.g., speeds). Despite these variations, some consistency appears that causes us to identify walking as belonging to the same class.

The fact that such variations exist within a single class of walking indicates the presence of redundancy in the system. That is, the presence of additional degrees of freedom allow the constraints induced by these various factors to be satisfied, while satisfying some underlying consistent behavioural goal. The latter could be to minimise effort, maintain comfort, or other such criteria. This dependence on the various factors makes modelling human gait hard in general [1], [2], especially given the fact that the precise influence of different factors on the movement can be hard to assess (e.g., how is the foot placement affected by different terrain [3], [4]).

Examples in modelling human gaits can be found in exoskeleton systems such as the Lokomat, the Skywalker, and the LOPES [5]–[7]. Although these devices are cleverly designed, much work is needed to personalise gait correction. One current issue is that existing systems normally restrict the patients to follow some predefined walking patterns, such that the patients are required to walk at certain speed, slope, or step size. However, clinical results show that motivating the patients to walk more proactively at a preferred pace promotes the overall results of rehabilitation [8]. Also, the pre-defined walking patterns are normally derived by taking an average gait template from healthy subjects, but it seems inadequate. For instance, this approach would consider faster or slower walks as deviations from a normal gait.

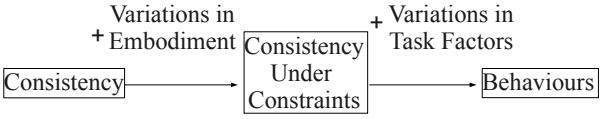

Fig. 1: Assuming the behaviours are the combination of consistent characteristics and variations in embodiment and task, we aim to recover the consistency by observing behaviours.

Some existing devices have a more flexible approach by incorporating impedance control and/or tolerating small deviation from the reference gait [9]–[11]. However, taking the average template framework as the reference is still problematic. Instead of restricting the patients to follow these predefined rules of training, a more appropriate way is to let the patients walk the way they prefer and correct them only if needed. Our approach is different from the previous work in that we aim to extract the consistent aspect of normal gaits and separate those from the natural variations (from embodiments and behaviours).

Our assumption is built upon previous research in gait analysis. Studies have shown small variations when performing the same gait. For example, [12] evaluated the repeatability of kinematic data of 40 subjects. Although there was variance in the range of motion, the kinematic patterns in the sagittal plane were highly predictable. [13] showed that, while EMG signals varied significantly when walking at different speeds, using PCA [14], just the first five principle components of these EMGs could account for the main features of the signals.

In recent years, a number of new tools have become available in the learning and robotics community that allow data from constrained and/or redundant systems [15], [16] to be used to uncover underlying consistent behaviours that may be otherwise masked by the constraints. Our approach is based on examining behaviours in the light of such methods, to see if certain underlying characteristics of gait can be found in the face of variations in embodiment and task factors (Fig. 1).

In this paper, we narrowed down our problem to a single class of human locomotion and analyse walking gaits on even terrain. We examine various walking behaviours across persons within this class and see if any consistency can be found. Potential applications of our work include rehabilitation, for example, through use of robotic support systems,

[1]Hsiu-Chin Lin and Sethu Vijayakumar are with the School of Informatics, University of Edinburgh, Edinburgh, UK H.Lin-21@sms.ed.ac.uk

[2]Matthew Howard is with the Department of Informatics, King's College London, London, UK

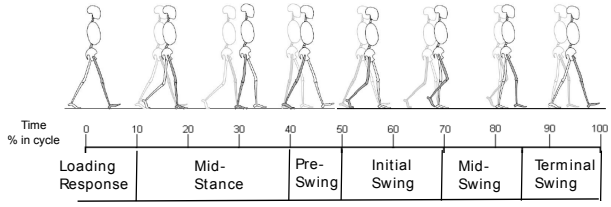

Fig. 2: Walking cycle and phases (extracted from [18])

and gait abnormality detection and diagnosis [5], [6], [17].

II. Walking Phase Models

A common approach in the gait analysis literature [18] is to decompose walking into a series of *cycles*, and a cycle can be further divided into a series of *phases* (Fig. 2). We assume that movements within each phase are the result of a composition of components handling the *phase critical components* of the motion (i.e., those must be controlled for successful completion of a given phase), and components that control the consistent aspects of the motion. In order to satisfy the phase critical components, it is assumed that a set of constraints

$$\mathbf{A}_k(\mathbf{x},t)\,\mathbf{u}(\mathbf{x},t) = \mathbf{b}_k(\mathbf{x},t) \tag{1}$$

is maintained, where $\mathbf{x} \in \mathbb{R}^n$ represents state, $\mathbf{u} \in \mathbb{R}^m$ represents action, t is time, and k indexes the phase. Here, the *task-space policy* $\mathbf{b}_k(\mathbf{x},t) \in \mathbb{R}^p$ $(p < m)$ describes a *task-dependent* control policy. The *constraint matrix* $\mathbf{A}_k(\mathbf{x},t) \in \mathbb{R}^{p\times m}$ is a matrix projecting $\mathbf{b}_k$ onto the relevant part of the control space. Inverting Eq. 1 results in the relation

$$\mathbf{u}(\mathbf{x},t) = \mathbf{A}_k(\mathbf{x},t)^\dagger\,\mathbf{b}(\mathbf{x},t) + \mathbf{N}_k(\mathbf{x},t)\,\boldsymbol{\pi}(\mathbf{x}) \tag{2}$$

where $\mathbf{A}^\dagger$ is the Moore-Penrose pseudo-inverse of $\mathbf{A}$, and we define $\mathbf{N}_k(\mathbf{x},t) := (\mathbf{I} - \mathbf{A}_k(\mathbf{x},t)^\dagger\,\mathbf{A}_k(\mathbf{x},t)) \in \mathbb{R}^{m\times m}$ where $\mathbf{I} \in \mathbb{R}^{m\times m}$ is the identity matrix. In Eq. 2, the second term arises due to the redundancy (since $p < m$), and allows control objectives to be realised through policy $\boldsymbol{\pi}(\mathbf{x}) \in \mathbb{R}^m$, subject to the constraints.

We assume that $\mathbf{A}_k$ and $\mathbf{b}_k$ are not explicitly known, but the quantities vary across walking phases to handle different phase critical components. We assume that $\boldsymbol{\pi}$ is *independent* of the phase; however, the *observed effects* of control toward these objectives (i.e., the motion $\mathbf{N}_k\,\boldsymbol{\pi}$) may be influenced by the phase. This is because the policy $\boldsymbol{\pi}$ is subject to the constraints imposed by different $\mathbf{A}_k$ and $\mathbf{b}_k$.

A. Decomposition of walking gait

We assume that the walking is a combination of *characteristics* of the gait and *variations* resulting from embodiments and behaviours. Here, we describe how to formulate the characteristics and variations with our walking-phase model.

1) Characteristics of walking: We hypothesise that there exists some consistent characteristics within a single class of human locomotion, such consistency may include energy minimisation, or maintenance of a comfort posture. The consistent characteristics of walking is captured in our model as the underlying null-space policy $\boldsymbol{\pi}$.

TABLE I: Correspondence between variations in walking gaits and the variables in our proposed model

Controlled Variables		Affected Variables	
Variation	Example	$\mathbf{b}$	$\mathbf{A}$
behaviour	speed, step-size	✓	
embodiments	leg-length		✓
phase			✓

An example of such a policy can be a limit cycle policy $\dot{r} = r(\rho - r^2), \dot{\theta} = \omega$ where r and θ are the polar representation of the state such that $\mathbf{x} = (r\cos(\theta), r\sin(\theta))^\top$, ρ is the radius of the attractor, and ω is the angular velocity.

2) Variations in embodiments: The variations in embodiments arise from inter-personal differences in factors such as body size, body type, and physical limits. In our model, such variations will result in modifications of the *constraint matrix* $\mathbf{A}$. (Hence, $\mathbf{A}$ varies across phases and subjects.)

In Eq. 1, we define the constraint matrix $\mathbf{A} \in \mathbb{R}^{p\times m}$ as a set of p *task-constraints*, and each task constraint refers to restrictions on the freedom of some subspace of the system. The task-constraints can be imposed in different representations (i.e., joint-space, end-effector space, etc).

A simple case is to restrict some sub-space of the joint-space. For example, if the state is defined as $\mathbf{x} = (q_1, q_2)^\top$, and the constraint matrix is set as $\mathbf{A} = (0, 1)$, the knee angle is restricted to follow various task-space policy $\mathbf{b}$ while the hip angle is free to move with the nullspace policy $\boldsymbol{\pi}$.

3) Variations in behaviours: The variations in behaviours are caused by other contextual factors such as the need to hurry for a meeting, and result in variations in, for example, step sizes and speeds. In our model, these variations are captured by the *task-space policy* $\mathbf{b}$, and we assume that $\mathbf{b}$ may vary across cycles to handle different behaviours.

In Eq. 1, we define the task-space policy $\mathbf{b} \in \mathbb{R}^p$ outputs the task-space velocity, in order to accomplish some operations. Depending on which dimension is constrained (i.e., defined by $\mathbf{A}$), the constrained dimensions are restricted to move to a specific target along that dimension.

For instance, in the terminal swing phase, the foot is placed on the ground at the end of the phase. $\mathbf{A}$ may be defined such that the foot position is controlled, while $\mathbf{b}$ may describe a point attractor driving the foot to a desired placement. An example of $\mathbf{b}$ could be a point-attractor $\mathbf{b}(\xi) = \alpha(\xi^* - \xi)$ where α is a parameter that controls the speed, ξ^* is the task-space target, and ξ is the task-space state. The position of heel strike depends on the step-length of that cycle; in this case, ξ^* can vary to handle different step-lengths.

Table I shows how the variations in walking (i.e., embodiments, behaviours, phases) affect the variables $\mathbf{A}$ and $\mathbf{b}$ in our walking phase model. Fig. 3 shows the correspondence between walking gaits and the walking-phase model. The observed behaviours $\mathbf{u}$ are the result of some consistent policy $\boldsymbol{\pi}$ modulated by various $\mathbf{A}$ and $\mathbf{b}$. With this formulation, we examine various $\mathbf{u}$ and see if $\boldsymbol{\pi}$ can be recovered.

B. Representations of human gait

Our walking phase model is generic and can be applied on different representations. For instance, in many motor control

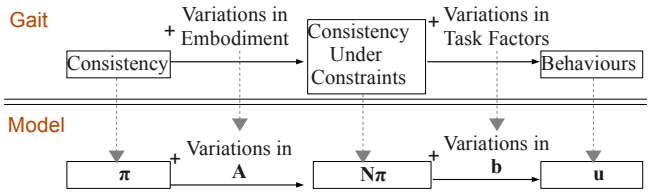

Fig. 3: Correspondence between walking gaits and model

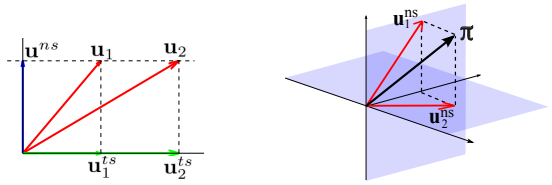

Fig. 4: A schematic of (a) Step-1 and (b) Step-2 of the proposed learning algorithm

problems, the system is typically characterised by joint-space and end-effector space [19]. For kinematic control, the state of the system can be represented by the joint-angles, and the controls can be the joint-velocities.

Aside from kinematic representations, several previous works have focused on using zero moment point (ZMP) to model humanoid locomotion [20]–[22]. Also popular are dynamical systems based representations of periodic movements [23], which have significant merits over time indexed representations. [24] is based on a periodic pattern generator and a coupled oscillator model to modulate the phase of sinusoidal patterns, in addition to representations that are derived from central pattern generators [25], [26].

In this paper, we focus on the kinematic representation of hip and knee joints, with the aim to explore more degrees-of-freedom and kinetic features in subsequent investigations.

III. Generalising Periodic Gaits

In this section, we describe our approach to generalising the characteristics of walking by learning a policy. Our method works on data given as $\mathcal{I}$ pairs of states $\mathbf{x}$ and actions $\mathbf{u}$. We assume that (i) $\mathbf{u}$ can be decomposed as $\mathbf{u}=\mathbf{A}^\dagger\,\mathbf{b}+\mathbf{N}\,\boldsymbol{\pi}$, (ii) $\mathbf{u}$ are generated using the same nullspace policy $\boldsymbol{\pi}$, (iii) $\mathbf{A}\,\mathbf{u}=\mathbf{b}$ for some $\mathbf{A}\neq 0$ and $\mathbf{b}\neq 0$, and (iv) $\mathbf{A}$, $\mathbf{b}$, and $\mathbf{N}$ are not explicitly known. The goal is to approximate the policy $\boldsymbol{\pi}$, that characterises the gait.

A. Naive (Average Template) Approach

A naive approach is to apply direct regression to estimate the policy. Note that, this corresponds to the default *average template* solution used in many gait and rehabilitation analysis. Specifically, one may minimise the error

$$E_{DPL}=\sum_{i=1}^{\mathcal{I}}||\mathbf{u}_i-\tilde{\boldsymbol{\pi}}_i||^2 \tag{3}$$

where $\tilde{\boldsymbol{\pi}}$ is some suitable estimator of the policy function. Such an approach ignores the variations in constraints $\mathbf{A}$ and task-space policy $\mathbf{b}$, and yields the average motion. However, this is unrealistic in everyday behaviour, so minimising Eq. 3 is unlikely to result in a good model.

B. Nullspace policy learning for periodic gaits

We take an alternative approach, in which the constraint and task space variations are explicitly considered. The proposed approach builds on previous research on policy recovery [16] for point-to-point movements, and adapts it to generalise the characteristics of gaits. The additional challenges in walking are (i) the differences due to interpersonal variations and (ii) the temporal switching of constraints between phases.

In the proposed approach, the policy $\boldsymbol{\pi}$ is estimated using two separate steps. The first step is to decompose the observations $\mathbf{u}$ into two orthogonal components: the task-space component $\mathbf{u}^{\text{ts}}\equiv\mathbf{A}^\dagger\,\mathbf{b}$ and the null-space component $\mathbf{u}^{\text{ns}}\equiv\mathbf{N}\,\boldsymbol{\pi}$ such that $\mathbf{u}=\mathbf{u}^{\text{ts}}+\mathbf{u}^{\text{ns}}$. The second step is to reconstruct the nullspace policy $\boldsymbol{\pi}$ from the estimated $\mathbf{u}^{\text{ns}}$. The following describes the two steps in detail.

1) Step-1 - Learning null-space component: The first step is to extract the null-space component $\mathbf{u}^{\text{ns}}$ from the raw observations $\mathbf{x},\mathbf{u}$. As discussed in [16], a requirement on this step is that the data are grouped into multiple subsets such that the constraint matrix $\mathbf{A}$ is consistent within each subset. In the present setting, this separation arises naturally from consideration of different subjects and phases.

Specifically, given input as pairs of states and actions $\mathbf{D}=\{\mathbf{x},\mathbf{u}\}$, the data is divided into $\mathcal{S}$ subsets such that subset $\mathbf{D}_s$ is the observations from subject s. Then, each $\mathbf{D}_s$ is further divided into $\mathcal{K}$ subsets $\mathbf{D}_{s,k}=\{\mathbf{x}_{s,k},\mathbf{u}_{s,k}\}$ where $k=1,2,...,\mathcal{K}$ is the phase number. For the $(s,k)^{th}$ subset, we seek a model that minimises the inconsistency between the true nullspace component $\mathbf{u}^{ns}_{s,k}$ and the estimated nullspace component $\tilde{\mathbf{u}}^{ns}_{s,k}$.

$$E[\mathbf{u}^{ns}_{s,k},\tilde{\mathbf{u}}^{ns}_{s,k}]=\sum_{i=1}^{\mathcal{I}_{s,k}}\left|\left|\mathbf{u}^{ns}_{s,k,i}-\tilde{\mathbf{u}}^{ns}_{s,k,i}\right|\right|^2 \tag{4}$$

Since we do not have access to the true null-space component $\mathbf{u}^{ns}_{s,k}$, Eq. 4 cannot be directly optimised. Instead, we attempt to eliminate the components of motion that are due to the task constraints, and learn a model that is consistent with the observations. To achieve this, we seek a projection matrix $\mathbf{P}_{s,k}=\tilde{\mathbf{u}}^{ns}_{s,k}\,\tilde{\mathbf{u}}^{ns}_{s,k}{}^\top/\left|\left|\tilde{\mathbf{u}}^{ns}_{s,k}\right|\right|^2$ which projects $\mathbf{u}_{s,k}$ onto the learnt nullspace component and satisfies $\mathbf{P}_{s,k}\,\mathbf{u}_{s,k}\equiv\mathbf{P}_{s,k}(\mathbf{u}^{ts}_{s,k}+\mathbf{u}^{ns}_{s,k})=\tilde{\mathbf{u}}^{ns}_{s,k}$. The objective function Eq. 4 can be rewritten as:

$$E_1[\tilde{\mathbf{u}}^{ns}_{s,k}]=\sum_{i=1}^{\mathcal{I}_{s,k}}\left|\left|\frac{\tilde{\mathbf{u}}^{ns}_{s,k,i}(\tilde{\mathbf{u}}^{ns}_{s,k,i})^\intercal}{\left|\left|\tilde{\mathbf{u}}^{ns}_{s,k,i}\right|\right|^2}\mathbf{u}_{s,k,i}-\tilde{\mathbf{u}}^{ns}_{s,k,i}\right|\right|^2 \tag{5}$$

Fig. 4a illustrates an example of this idea. Assuming there are two observation $\mathbf{u}_1$, $\mathbf{u}_2$ from the same $\mathbf{x}$ within a subset. Since the constraint is consistent, $\mathbf{u}_1$, $\mathbf{u}_2$ must have the same $\mathbf{u}^{\text{ns}}$. We seek a $\mathbf{u}^{\text{ns}}$ such that when $\mathbf{u}_1$ and $\mathbf{u}_2$ are projected onto $\mathbf{u}^{\text{ns}}$, the error is minimised.

In this paper, each $\tilde{\mathbf{u}}^{ns}_{s,k}$ is modelled through iterative optimisation of Eq. 5 using Gaussian radial basis functions.

Algorithm 1 Null-space Policy Learning

Input: $\mathbf{D} = \{\mathbf{x}, \mathbf{u}\}$: data-set of states $\mathbf{x}$ and action $\mathbf{u}$
Output: $\tilde{\boldsymbol{\pi}}$: learnt null-space policy

```
Split D into D_s where D_s is the input from subject s
Split D_s into D_{s,k} where k denotes the phase number
for all D_{s,k} do
    Learn ũ^{ns}_{s,k} by minimising Eq. 5
end for
Combine {x_{s,k}, ũ^{ns}_{s,k}} into a single data-set {x, ũ^{ns}}
Learn π̃ by minimising Eq. 7
```

More precisely, $\tilde{\mathbf{u}}^{ns}_{s,k} = \mathbf{W}_{s,k}\, \boldsymbol{\beta}(\mathbf{x}_{s,k})$ where $\mathbf{W}_{s,k} \in \mathbb{R}^{m \times \mathcal{J}}$ is a matrix of weights, and $\boldsymbol{\beta}(\mathbf{x}_{s,k}) = \frac{K(\mathbf{x}_{s,k} - \mathbf{c}_j)}{\sum_{j=1}^{\mathcal{J}} K(\mathbf{x} - \mathbf{c}_j)} \in \mathbb{R}^{\mathcal{J}}$ is a vector of basis functions, $\mathcal{J}$ is the number of basis functions, and $\mathbf{c}_j$ for $j = 1, ..., \mathcal{J}$ are the centres. The optimisation is initialised using direct regression to find the initial approximation $\mathbf{W}^0_{s,k} = \arg\min \sum \left|\left| \mathbf{u}_{s,k} - \tilde{\mathbf{u}}^{ns}_{s,k} \right|\right|^2$.

2) Step-2 - Learning null-space policies: The output of Step-1 is a set of $s \times k$ intermediate models for the nullspace component $\tilde{\mathbf{u}}^{ns}_{s,k} \approx \mathbf{N}_{s,k}\, \boldsymbol{\pi}$. The goal of Step-2 is to approximate policy $\tilde{\boldsymbol{\pi}}$ that is consistent with all $\tilde{\mathbf{u}}^{ns}_{s,k}$. Ideally, the approximation should minimise the error between the true policy and the learnt policy

$$E[\boldsymbol{\pi}, \tilde{\boldsymbol{\pi}}] = \sum_{i=1}^{\mathcal{I}} ||\boldsymbol{\pi}_i - \tilde{\boldsymbol{\pi}}_i||^2. \tag{6}$$

Unfortunately, since the true policy $\boldsymbol{\pi}$ is not observed, Eq. 6 cannot be minimised directly. Instead, we proceed by noting that, on completion of Step-1 we have the equivalent to a set of $s \times k$ systems that satisfy $\mathbf{A}_{s,k}\, \tilde{\mathbf{u}}^{ns}_{s,k} = 0$. As a result we can adapt the work in [15] to find a policy that is maximally consistent with the observations. More precisely, the $s \times k$ intermediate models are combined into a single data set $(\mathbf{x}, \tilde{\mathbf{u}}^{ns})$, and the approximation is made by minimising

$$E_2[\tilde{\boldsymbol{\pi}}] = \sum_{i=1}^{\mathcal{I}} \left|\left| \frac{\tilde{\mathbf{u}}^{ns}_i\, \tilde{\mathbf{u}}^{ns\,\top}_i}{||\tilde{\mathbf{u}}^{ns}_i||^2}\, \tilde{\boldsymbol{\pi}}(\mathbf{x}_i) - \tilde{\mathbf{u}}^{ns}_i \right|\right|^2 \tag{7}$$

An example is illustrated in Fig. 4b. Given two nullspace components $\mathbf{u}^{ns}_1$ and $\mathbf{u}^{ns}_2$, the inconsistency error favours models for which there is minimal discrepancy between $\mathbf{u}^{ns}_1$ and $\mathbf{u}^{ns}_2$ and the model, projected onto these observations.

The nullspace policy $\tilde{\boldsymbol{\pi}}$ can be modelled with Gaussian radial basis functions, through minimisation of Eq. 7. The entire process of recovering $\boldsymbol{\pi}$ is summarised in Algorithm 1.

IV. Identifying pathological gaits

One of our objectives is to quantify the difference between gaits, and a potential application is gait abnormality detection. The principle is to compare an unknown gait with a reference gait which is expected to be normal, and use their difference as the classification criteria.

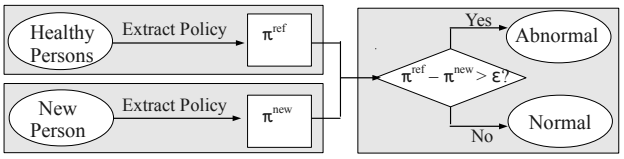

Fig. 5: Gait abnormality detection by measuring the difference in nullspace policies

A. Quantifying Difference between Gaits

With our model, comparing two gaits is equivalent to comparing two nullspace policies. A general framework is illustrated in Fig. 5; ideally, we want to extract the nullspace policy from healthy subjects (reference policy $\boldsymbol{\pi}^{ref}$) and compare to the nullspace policy from a new subject ($\boldsymbol{\pi}^{new}$). A difference above a certain threshold would signify a pathological gait.

However, in order to estimate $\boldsymbol{\pi}^{new}$, observations from various embodiments are required, which is infeasible for the new subject. Nevertheless, it is still possible to detect abnormalities in gait by comparing the policies *under constraints*. Specifically, instead of measuring the difference between $\boldsymbol{\pi}^{new}$ and $\boldsymbol{\pi}^{ref}$, we evaluate the difference between $\mathbf{N}^{new}\, \boldsymbol{\pi}^{new}$ and $\mathbf{N}^{new}\, \boldsymbol{\pi}^{ref}$, where $\mathbf{N}^{new}$ is a projection matrix derived from the constraints of the new subject.

B. Projection Matrix Estimation

The projection matrix of the new person $\mathbf{N}^{new}$ is unavailable by assumption, but it is possible to estimate it. By definition, $\mathbf{u}^{\text{ns}} = \mathbf{N}\, \boldsymbol{\pi}$ where $\mathbf{N}$ is the projection matrix which projects a vector onto the image space of $\mathbf{N}$. Since $\mathbf{u}^{\text{ns}}$ is already in the image space of $\mathbf{N}$, we must have $\mathbf{N}\, \mathbf{u}^{\text{ns}} = \mathbf{u}^{\text{ns}}$.

Based on this insight, an estimate of the projection matrix can be found by searching over the range of possible projections. Recall that $\mathbf{N} = \mathbf{I} - \mathbf{A}^{\dagger}\, \mathbf{A}$; hence, we need to find an $\mathbf{A}$ that matches the direction of the constraint as closely as possible. In this paper, we have constraints $\mathbf{A} \in \mathbb{R}^{1 \times 2}$, so we can model the constraint as a unit vector $\tilde{\mathbf{A}} = [\cos(\theta)\, \sin(\theta)]$, where $\theta \in [0, \pi]$ covers all possible cases of $\mathbf{N}$.

For the k^{th} phase of a new person, we seek a θ_k such that the difference between $\tilde{\mathbf{N}}^{new}_k\, \mathbf{u}^{ns,new}_k$ and $\mathbf{u}^{ns,new}_k$ is minimised. Note that the true nullspace component of the new subject $\mathbf{u}^{ns,new}_k$ is also unknown, so we use the *estimated nullspace component*, instead.

Namely, after learning the nullspace component $\tilde{\mathbf{u}}^{ns,new}_k$ for the k^{th} phase, we obtained $\mathcal{I}_k$ pairs of $(\mathbf{x}_k, \tilde{\mathbf{u}}^{ns,new}_k)$. For each possible value of $\theta_k \in [0, \pi]$, we can calculate the difference between $\tilde{\mathbf{N}}^{new}_k\, \tilde{\mathbf{u}}^{ns,new}_k$ and $\tilde{\mathbf{u}}^{ns,new}_k$

$$E_\theta[\tilde{\mathbf{N}}^{new}_k] = \sum_{i}^{\mathcal{I}_k} \left|\left| \tilde{\mathbf{N}}^{new}_k\, \tilde{\mathbf{u}}^{ns,new}_{k,i} - \tilde{\mathbf{u}}^{ns,new}_{k,i} \right|\right|^2. \tag{8}$$

The optimal $\theta_k \in [0, \pi]$ minimises Eq. 8

C. Approximate policy difference

The difference between the new person and the reference is quantified through *approximate constrained policy difference*

Algorithm 2 Approximate difference between two gaits

Input: $\mathbf{D} = \{\mathbf{x}^{new}, \mathbf{u}^{new}\}$: data-set of a new person
$\boldsymbol{\pi}^{ref}$: reference policy
Output: APD: approximated policy difference
1: Split $\mathbf{D}$ into $\mathbf{D}_k$ where k denotes the phase number
2: **for all** $\mathbf{D}_k$ **do**
3: Learn $\tilde{\mathbf{u}}_k^{ns,new}$ by minimising Eq. 5
4: Learn $\tilde{\mathbf{N}}_k^{new}$ by minimising Eq. 8
5: **end for**
6: Approximate the difference using Eq. 9

(a) (b) (c) (d)

Fig. 6: Kinematic data was collected using (a) Motion Analysis Eagle-4 in the University of Tokyo and (b) Xsens MVN BIOMECH in the University of Edinburgh. In (c) Tokyo Data and (d) Edinburgh Data, extra weight was attached to the subjects to create 'abnormal' gaits.

(APD). Specifically, given pairs of state/action of the new person $\mathbf{x}^{new}, \mathbf{u}^{new}$, we divide their data into $\mathcal{K}$ walking phases and learn the nullspace components $\tilde{\mathbf{u}}_k^{ns,new}$ for each phase. Then, we take $\tilde{\mathbf{u}}_k^{ns,new}$ to estimate projection matrix $\tilde{\mathbf{N}}_k^{new}$ using Eq. 8. The APD is computed as

$$APD = \frac{1}{\mathcal{I}\sigma^2_{\boldsymbol{\pi}^{ref}}} \sum_{k=1}^{\mathcal{K}} \sum_{i=1}^{\mathcal{I}_k} \left|\left| \tilde{\mathbf{u}}_{k,i}^{ns,new} - \tilde{\mathbf{N}}_k^{new} \boldsymbol{\pi}_{k,i}^{ref} \right|\right|^2 \quad (9)$$

where $\mathcal{I} = \sum_k \mathcal{I}_k$ and $\sigma^2_{\boldsymbol{\pi}^{ref}}$ is the variance of the reference policy. The APD measures the difference between the reference policy and the new person in the constrained space, normalised by the variance of the reference policy.

Eq. 9 can be interpreted as the difference between a person and the reference where the distance resulting from various behaviours (speeds, step-sizes) is eliminated. Therefore, this measurement can be thought of as the quantification of how much we should correct a gait without interfering with speed or step-length. Additionally, the APD can be used for monitoring a program of rehabilitation by looking at the evolution of the APD with training. Algorithm 2 summarises the process.

V. Experiment on Human Data

In this experiment, we used motion-capture data to test (i) how well our method can recover the policy and (ii) how well we can employ the learnt policy for gait abnormality detection.

TABLE II: Leg lengths of the subjects

Subject	Upper Leg (cm)	Lower Leg (cm)	Data-set
S1	37.7	38.9	Tokyo
S2	41.6	41.1	Tokyo
S3	44.2	43.3	Tokyo
S4	42.6	40.5	Edinburgh
S5	45.1	44.2	Edinburgh
S6	42.5	41.5	Edinburgh
S7	45.8	44.8	Edinburgh

A. Data Collection

Kinematic data was obtained from two separate sources. The first data-set was collected with a Motion Analysis Eagle-4 system [27] in the University of Tokyo (Tokyo Data). The system is consisted of 10 cameras recording at a frame rate of 200fps (Fig. 6a), and the motion capture was performed with 35 optical markers placed on the subject.

The second data-set was collected using Xsens MVN BIOMECH system [28] in the University of Edinburgh (Edinburgh Data). The sensor units were attached to the subjects according to Xsens configuration (Fig. 6b). The update frequency is set to 120 FPS.

1) Variations: The data were collected from seven males, age between 20-29 (referred as S1-S7). Three subjects (S1-S3) were collected in University of Tokyo, and four subjects (S4-S7) were collected in the University of Edinburgh. These seven subjects have different body types, and they were chosen to ensure our data contains some variations in embodiments. The leg-lengths of the subjects are summarised in Table. II.

Data was recorded for five walking speeds: 93, 106, 119, 129, 140 steps per minute, which were taken from the speed range reported in [29]. The walking speeds were controlled through use of a metronome. The subjects were asked to walk such that heel strike coincided with the tick of the metronome. For each speed, ten walking trials were collected.

2) Pathological gait: Extra weight was attached to the subjects to alter their walking patterns. In Tokyo Data, a 1 kg bottle was strapped to the subjects' left shank (Fig. 6c). In Edinburgh Data, 3.5 kg bags of sand was strapped to the subjects' left ankle (Fig. 6d). We used the same setup (speeds, trail size, etc) to collect abnormal gait from each subject.

3) Pre-processing: We used heel-strike of the left leg to demark the beginning of a gait cycle and extracted as many cycles as possible from all walking trails we collected. We obtained roughly 200 gait cycles from each subject, and 100 cycles were selected for analysis. Fig. 7 shows the hip and knee angle from one of the subjects. One trajectory from each speed was selected. Note that normal gaits (red) and abnormal gaits (black) look very similar from direct observation.

B. Setup

1) Representation: In this experiment, we analysed the sagittal plane kinematics of the hip and knee joints. For this,

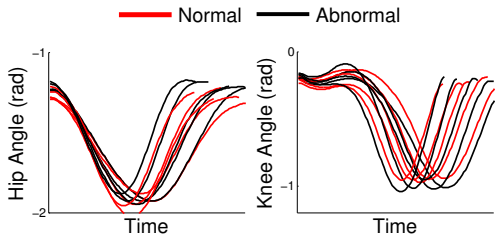

Fig. 7: The normal gait and abnormal gait from one subject

the state and action spaces were described by the joint-angles $\mathbf{x} \in \mathbb{R}^2$ and joint-velocities $\mathbf{u} \in \mathbb{R}^2$, respectively.

2) Phase Division: Each walking cycle is divided into three phases: (i) stance, (ii) pre-swing and initial swing, and (iii) mid-swing and terminal swing. Note that using three phases is not conventional or necessarily optimal. However, this seems to be the smallest sub-divisions of the walking cycle that guarantees a consistent constraint $\mathbf{A}_k$ across the entire k^{th} phase, which is a condition for our method to be effective.

3) Learning reference policy: We selected five subjects, S1-S5, for learning the reference policy (Alg. 1). For each walking phase of each subject, we learnt the nullspace component $\tilde{\mathbf{u}}_{s,k}^{ns,ref}$, which yielded 15 models. Each $\tilde{\mathbf{u}}_{s,k}^{ns,ref}$ consisted of $\mathcal{J}$ Gaussian RBFs where $\mathcal{J}$ varied from 16 to 100. From the set of $\tilde{\mathbf{u}}_{s,k}^{ns,ref}$, we learnt the nullspace policy $\boldsymbol{\pi}^{ref}$, which was also modelled with Gaussian RBFs. We used this learnt policy as the reference policy in all experiments.

4) Identify pathological gaits: Five subjects (S1-S5) were used to collect five normal and five pathological gaits (using the leg loading). To investigate how well the learnt policy can generalise across subjects, we also performed the same experiment on the subjects whose data had not been used for training the reference policy (S6-S7) – we collected normal and pathological gaits for each of these. Alg. 2 was applied on each person separately. Namely, we learnt the $\tilde{\mathbf{u}}_k^{ns,new}$ for each phase of each person. The differences between each person and the reference were calculated using APD (Eq. 9).

5) Baseline: For comparison, we also trained models using (i) linear regression and (ii) RBF network on raw observations $(\mathbf{x}, \mathbf{u})$ from the normal gaits, and tested if we can see a difference between normal and abnormal gaits in joint-space.

C. Results

The average results over all subjects are shown in Fig. 8. The y-axis shows the average differences in joint-space for the regression methods and the average APD for the proposed method. (Note that, the proposed method attempts to eliminate the difference resulting from various walking behaviours; therefore, our method does not directly compare joint-angles, which may be influenced by behaviours.)

Fig. 8a shows the average results over S1-S5. We can see that the standard methods (yellow and green) cannot differentiate normal and abnormal gait. Our approach (red) achieved relatively lower difference when comparing with

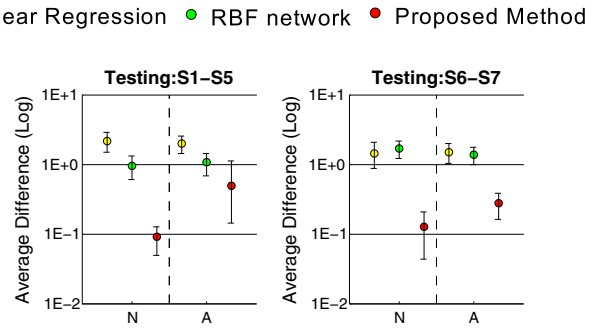

Fig. 8: Average difference between the testing subjects and the reference. The testing subjects are (a) S1-S5 and (b) S6-S7. The results were grouped into normal (N) and abnormal (A). The error-bars are mean±std.dev. in log-scale over ten experiments.

normal gaits and higher difference when comparing with abnormal gaits. Even if we have no access to the true policy, constraints, nor tasks, our reference policy is more effective in differentiating normal and abnormal.

Fig. 8b shows the the average results over S6 and S7. In this case, the RBF network (green) predicts that the abnormal gait is more similar to the reference gait. This outcome reflects the problem of using average templates, where the reference gait fails to adapt to the new subjects. Our proposed method (red), on the other hand, shows greater difference for the abnormal gait, even though S6 and S7 are different from the subjects used to train the reference policy.

1) Apply the learnt policies on various behaviours: We also evaluated how well the learnt policies can generalise across various walking behaviours. In this experiment, we tested slow, average, and fast walks separately, to see how the results might be affected by various speeds.

Similar to the last experiment, we used the normal and abnormal gait from S6 and S7 to represent two normal and two abnormal persons, and compare them with the reference policy learnt from S1-S5. Fig. 9 shows the results of the predicted difference between the new subjects and the reference, where the data was divided into: (a) slow, (b) average, and (c) fast.

From Fig. 9, we can see that, by using the RBF network (green), the predicted difference between the normal gait and the reference increases as the walking speed increases. This is equivalent to considering those faster walks are deviations from the normal gait. In contrast, our method (red) yields lower difference for normal compared to abnormal walking regardless of speed. This outcome confirms the fact that our method eliminates the difference coming from various walking speeds. The implication in a real world application is that, our method deals with different walking behaviours consistently, and the patients can choose to walk faster or slower.

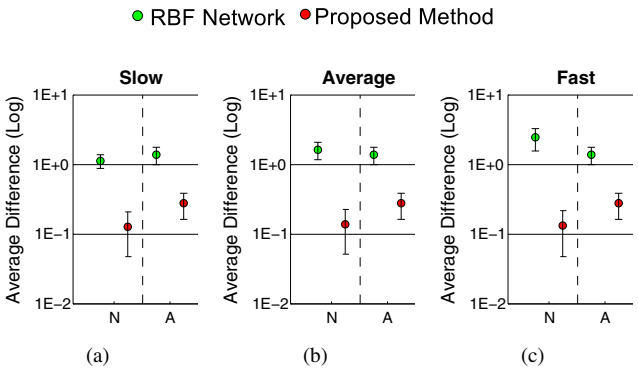

Fig. 9: Predicted differences in joint-space between the testing subjects (S6-S7) and the reference (S1-S5). The testing data was divided into (a) slow, (b) average, and (c) fast

VI. Conclusion

We explore the problem of representing, generalising, and comparing gaits. We consider that locomotion can be described as a combination of characteristics of the gait and variations from embodiments and behaviours. We assume that characteristics are consistent across embodiments and behaviours, and we aim to generalise them.

We formulate our problem into a walking phase model, and we adapt the nullspace policy learning method to generalise a policy that can capture the consistent characteristics of walking gait. Our experiment has shown that our method is effective in reconstructing the policy, and we can utilise this recovered policy for gait abnormality detection.

We analysed the kinematics of movement in this paper, and future work will focus on exploring different representations and higher degree-of-freedom. The success of our work is expected to promote better gait rehabilitation. In the future, we would like to use the reconstructed policy to produce the reference trajectory for gait rehabilitation. With our method, the system will be able to correct the patient only if there is a mismatch in the characteristics of walking without interfering his/her personal preferences such as speeds or step-lengths.

References

[1] F. Multon, L. France, M.-P. Cani-Gascuel, and G. Debunne, "Computer animation of human walking: a survey," *The Journal of Visualization and Computer Animation*, vol. 10, no. 1, pp. 39–54, 1999.

[2] R. Boulic, N. Thalmann, and D. Thalmann, "A global human walking model with real-time kinematic personification," *The Visual Computer*, vol. 6, pp. 344–358, 1990.

[3] D. Pongas, M. Mistry, and S. Schaal, "A robust quadruped walking gait for traversing rough terrain," in *International Conference on Robotics and Automation*, 2007, pp. 1474–1479.

[4] Y. Fukuoka, H. Kimura, and A. H. Cohen, "Adaptive dynamic walking of a quadruped robot on irregular terrain based on biological concepts," *The International Journal of Robotics Research*, vol. 22, no. 3-4, pp. 187–202, 2003.

[5] A. Duschau-Wicke, J. von Zitzewitz, A. Caprez, L. Lunenburger, and R. Riener, "Path control: A method for patient-cooperative robot-aided gait rehabilitationsky," *IEEE Transactions on Neural Systems and Rehabilitation Engineering*, vol. 18, no. 1, pp. 38 –48, 2010.

[6] P. Artemiadis and H. Krebs, "On the potential field-based control of the mit-skywalker," in *International Conference on Robotics and Automation*, 2011.

[7] J. Veneman, R. Kruidhof, E. Hekman, R. Ekkelenkamp, E. van Asseldonk, and H. van der Kooij, "Design and evaluation of the lopes exoskeleton robot for interactive gait rehabilitation," *IEEE Transactions on Neural Systems and Rehabilitation Engineering*, vol. 15, pp. 379–386, 2007.

[8] J. Hidler, D. Nichols, M. Pelliccio, and K. Brady, "Advances in the understanding and treatment of stroke impairment using robotic devices," *Topics Stroke Rehabilitation*, vol. 12, 2005.

[9] S. Jezernik, G. Colombo, and M. Morari, "Automatic gait-pattern adaptation algorithms for rehabilitation with a 4-dof robotic orthosis," *IEEE Transactions on Robotics and Automation*, vol. 20, no. 3, pp. 574–582, 2004.

[10] J. F. Veneman, R. Ekkelenkamp, R. Kruidhof, F. C. Van Der Helm, and H. Van Der Kooij, "A series elastic- and bowden-cable-based actuation system for use as torque actuator in exoskeleton-type robots," *International Journal Robotic Research*, vol. 25, pp. 261–281, 2006.

[11] R. Riener, L. Lunenburger, S. Jezernik, M. Anderschitz, G. Colombo, and V. Dietz, "Patient-cooperative strategies for robot-aided treadmill training: first experimental results," *IEEE Transactions on Neural Systems and Rehabilitation Engineering*, vol. 13, no. 3, pp. 380–394, 2005.

[12] V. Stokes, C. Andersson, and H. Forssberg, "Rotational and translational movement features of the pelvis and thorax during adult human locomotion," *Journal of Biomechanics*, vol. 22, no. 1, pp. 43–50, 1989.

[13] Y. P. Ivanenko, R. E. Poppele, and F. Lacquaniti, "Five basic muscle activation patterns account for muscle activity during human locomotion," *The Journal of Physiology*, no. 556, 2004.

[14] I. T. Jolliffe, *Principal components analysis*. Springer-Verlag, 1986.

[15] M. Howard, S. Klanke, M. Gienger, C. Goerick, and S. Vijayakumar, "A novel method for learning policies from variable constraint data," *Autonomous Robots*, vol. 27, pp. 105–121, 2009.

[16] C. Towell, M. Howard, and S. Vijayakumar, "Learning nullspace policies," in *International Conference on Intelligent Robots and Systems*, 2010.

[17] S. Lee and Y. Sankai, "Power assist control for walking aid with hal-3 based on emg and impedance adjustment around knee joint," in *International Conference on Intelligent Robots and Systems*, 2002.

[18] M. W. Whittle, *Gait analysis: an introduction*, 3rd ed. Oxford, United Kingdom: Butterworth-Heinemann, 2003.

[19] B. Siciliano and O. Khatib, *Springer Handbook of Robotics*. Secaucus, NJ, USA: Springer-Verlag New York, Inc., 2007.

[20] S. Kajita, F. Kanehiro, K. Kaneko, K. Fujiwara, K. Harada, K. Yokoi, and H. Hirukawa, "Biped walking pattern generation by using preview control of zero-moment point," in *International Conference on Robotics and Automation*, 2003.

[21] Y. Ogura, H. Aikawa, K. Shimomura, H. Kondo, A. Morishima, H. Lim, and A. Takanishi, "Development of a new humanoid robot wabian-2," in *International Conference on Robotics and Automation*, 2006.

[22] Y. Guan, E. S. Neo, K. Yokoi, and K. Tanie, "Stepping over obstacles with humanoid robots," *IEEE Transactions on Robotics*, vol. 22, pp. 958 –973, 2006.

[23] A. J. Ijspeert, J. Nakanishi, and S. Schaal, "Learning attractor landscapes for learning motor primitives," in *Advances in Neural Information Processing Systems*, 2003.

[24] J. Morimoto and C. Atkeson, "Nonparametric representation of an approximated poincaré map for learning biped locomotion," *Autonomous Robots*, vol. 27, pp. 131–144, 2009.

[25] A. Ijspeert and A. Crespi, "Online trajectory generation in an amphibious snake robot using a lamprey-like central pattern generator model," in *International Conference on Robotics and Automation*, 2007.

[26] Y. Nakamura, T. Mori, M. Sato, and S. Ishii, "Reinforcement learning for a biped robot based on a cpg-actor-critic method," *Neural Networks*, vol. 20, no. 6, pp. 723–735, 2007.

[27] MotionAnalysis, "Motion analysis corporation, the motion capture leader," http://www.motionanalysis.com, MotionAnalysis, 2012.

[28] D. Roetenberg, H. Luinge, and P. Slycke, "Xsens mvn: full 6 dof human motion tracking using miniature inertial sensors," Xsens Technologies BV, Enschede, The Netherlands, 2009.

[29] T. Öberg, A. Karsznia, and K. Öberg, "Basic gait parameters: reference data for normal subjects, 10-79 years of age," *Journal of rehabilitation research and development*, vol. 30, pp. 210–210, 1993.